Supplemental Materials
for

A novel "cut and paste" method for *in situ* replacement of cMyBP-C reveals a new role for cMyBP-C in the regulation of contractile oscillations

Nathaniel C. Napierski BS[1], Kevin Granger BS[1], Paul R. Langlais PhD[2], Hannah R. Moran BS[1], Joshua Strom PhD[1], Katia Touma MS[3], and Samantha P. Harris PhD[1]*

1) *Department of Cellular and Molecular Medicine, University of Arizona, College of Medicine, Tucson, Arizona, 85724-5044*
2) *Department of Medicine, Division of Endocrinology, University of Arizona, College of Medicine, Tucson, Arizona, 85724-5044*
3) *Roche Tissue Diagnostics, Tucson, Arizona, 85755*

Corresponding Author: Samantha P. Harris
Email: samharris@email.arizona.edu

This PDF file includes:

Expanded Materials and Methods
Major Resources Table
Online Figures I-VIII
Online Tables I-III
Major Resources Table
Legends for Online Videos I-VII

Other online supplementary materials for this manuscript include the following:

Online Videos I-VII
Online Tables (Excel files) IV-V

Expanded Material and Methods

Data that support the findings of this study are available from the corresponding author upon reasonable request. A list of major reagents and their sources can be found in the Major Resources Table at the end of the Online Supplemental Materials.

Animals. Treatment of all animals was in accordance with the National Research Council Guide for the Care and Use of Laboratory Animals using protocols approved by the Institutional Animal Care and Use Committee at the University of Arizona. Mice used for force measurements were treated with propranolol in their drinking water (0.5-1 g/L) for 4-7 days prior to euthanasia to prevent excess phosphorylation of cMyBP-C when euthanized[4]. Anesthetized mice were euthanized by cervical dislocation. To minimize the number of animals used for force measurements randomization with respect to genotype (blinding) was not done because the "cut and paste" method uses only homozygous myocytes and therefore more homozygous mice than wild-type mice were needed. Excised hearts were trimmed, weighed, and dissected left ventricles (LV) were flash frozen in liquid nitrogen prior to storage at -80^{o}C until use.

Gene-editing and generation of Spy-C mice. Spy-C mice were created by the GEMM core at the University of Arizona using CRISPR/Cas9 based gene-editing and Homology Directed Repair. Briefly, Spy-C mice were created by inserting a 60 nucleotide cassette into the *MYBPC3* gene locus (between domains C7 and C8 of the cMyBP-C protein) using a synthetic single guide RNA injected into fertilized mouse zygotes (strain Bl6/NJ). The 60 nucleotide insert encodes i) a TEVp consensus recognition sequence (ENLYFQG) followed by ii) a SpyTag sequence (AHIVMVDAYKPTK)[23]. 3 male Spy-C founder mice were obtained following gene-editing of zygotes; 2 males (7E and 2G) were homozygous for the insertion and 1 male (1F) was heterozygous for the insertion. All 3 males survived into adulthood, were fertile, and generated progeny that were maintained as separate founder lines. All founder lines produced offspring in

expected Mendelian inheritance ratios (Online Fig. I). Spy-C mice were inbred within their founder lines and were not backcrossed. Founder progeny were outbred with WT C57BL6/NJ mice from Jackson laboratories every 10 generations. cMyBP-C protein expression and echocardiography was analyzed independently for each line. No significant differences were observed between any of the 3 founder lines (not shown).

Echocardiography. Cardiac wall dimensions and functional parameters were measured by non-invasive echocardiography at the UArizona Mouse Phenotyping Core in male and female mice (8-52 weeks of age) of each founder line. Echocardiography was performed by a sonographer who was blinded to genotype with mice under mild sedation (1-3% isoflurane) as described previously[4]. All abbreviations for morphological and hemodynamic parameters are given in Online Table I.

cMyBP-C quantification and localization. Proteins were prepared for western blot analyses by pulverizing frozen LV and septum using a mortar and pestle cooled with liquid nitrogen. Pulverized tissue was held at -20°C for 20-60 min and solubilized in a urea buffer ([in mol/L]: 8 Urea, 2 Thiourea, 0.05 Tris-HCl, 0.075 dithiothreitol with 3% SDS and 0.03% Bromophenol blue pH 6.8) and 50% glycerol with protease inhibitors ([in mmol/L]: 0.04 E64, 0.16 Leupeptin and 0.2 PMSF) at 60°C for 10 min. Solubilized tissues were centrifuged, aliquoted and frozen prior to separation by gel electrophoresis (4-15% Mini-ProteanTGX, Biorad) and subsequent transfer to nitrocellulose membranes. Total cMyBP-C was quantified using primary antibodies to cMyBP-C[40] and α-actinin (mouse α-actinin antibody, Sigma-Aldrich A7811) or actin (Sigma A9357 monoclonal mouse anti-actin antibody) as a loading control. cMyBP-C antibody validation was described previously[24,40]. Secondary antibodies were goat anti-rabbit IRDye(r) 800CW (Li-Cor) and goat anti-mouse IRDye(r) 680CW (Li-Cor). A custom rabbit polyclonal antibody against the SpyTag sequence was obtained from GenScript USA (Piscataway, NJ). Specificity of the SpyTag antibody was verified on western blots showing bands at expected size pre and post TEVp digestion of HO myocytes (Fig. 2). Immunofluorescence localization of cMyBP-C in permeabilized myocytes was performed as

previously described with primary antibodies against cMyBP-C and α-actinin and secondary antibodies (goat anti-rabbit AlexaFluor488 for cMyCP-C (A11008, Invitrogen) and goat anti-mouse AlexaFluor568 for α-actinin (A11004, Life Technologies)[4].

Recombinant protein expression and purification. Recombinant proteins containing various cMyBP-C N'-terminal domains (murine cDNA sequence, NP_032679.2) and SpyCatcher [-sc][23] were cloned and expressed from a synonymous codon sequence optimized for expression in bacteria (GenScript, Piscataway, NJ). A plasmid encoding the TEV protease sequence pRK793 was a gift from David Waugh (Addgene plasmid #8827; http://n2t.net/addgene:8827; RRID:Addgene_8827)[66]. All recombinant proteins were expressed in BL21 DE3 (C2527H, NEB) in Overnight Express Instant TB medium (EMD Millipore) according to manufacturer's protocol. Purification of recombinant proteins was accomplished by hexahistidine tag using Ni-NTA resin (1018244, Qiagen) according to manufacturer's protocol.

For PKA phosphorylation, purified recombinant proteins were treated with protein kinase A (PKA, P2645 Sigma) by reconstituting 400U of PKA in Relax buffer with 4 mM $MgCl_2$ and 6 mM DTT and incubating with recombinant protein (10 mg) for 1 hr at room temperature. Phosphorylated protein was separated from PKA by a second affinity purification step using Ni-NTA as described above before use in force assays. Protein phosphorylation was confirmed by ProQ staining (P33301, Invitrogen). Briefly, samples of p-*r*C0C7-sc and untreated *r*C0C7-sc proteins were denatured and separated by SDS-PAGE. The gel was stained for phosphoproteins by ProQ Diamond (Invitrogen) gel stain according to manufacturer directions. Following imaging the same gel was stained by SYPRO Ruby total protein gel stain (Invitrogen) according to manufacturer directions and imaged again.

Cut and paste replacement of cMyBP-C N'-terminal domains in permeabilized myocytes. For batch removal and replacement of cMyBP-C N'-terminal domains in permeabilized myocytes from Spy-C mice, myocytes were prepared as described for force measurements and rinsed 3x in fresh relax buffer without

detergents. To remove genetically encoded (γ) domains C0C7 of endogenous cMyBP-C, myocytes were next incubated with purified recombinant TEVp (20 μM, 30 min at room temperature) followed by 3 rinses in fresh relax buffer to remove TEVp and γC0C7. Covalent ligation of new recombinant (*r*) cMyBP-C N'-terminal domains (with SpyCatcher (-sc) encoded at their C'-terminal ends) was achieved by incubating with 20 μM of the desired recombinant protein for 20 min. In some cases, TEVp treatment was omitted and recombinant proteins were directly added to permeabilized myocytes. Excess recombinant protein not covalently ligated to SpyTag (st) was removed by 3x washes in fresh relax buffer without added protein. Permeabilized myocyte samples were then dissolved in a urea sample buffer and analyzed by western blotting as described above. Efficiency of *r*C0C7-sc ligation was determined by densitometric analysis of western blot images using ImageJ[67]. Bands corresponding to ligated proteins were normalized to α-actinin or actin as a loading control and expressed as a percentage relative to the uncut cMyBP-C band (also normalized to α-actinin or actin) in control myocytes that had not been treated with TEVp.

Force measurements in permeabilized myocytes. Permeabilized multi-cellular myocyte preparations were prepared as described previously[68]. Briefly, frozen left ventricles were mechanically disrupted using a Polytron homogenizer (PT1200E, Kinematica) in a skinning solution (5.92 mM Na_2ATP, 6.04 mM $MgCl_2$, 2 mM EGTA, 139.6 mM KCl, 10 mM Imidazole, 0.01% saponin, 1% Triton-x-100®, Halt protease inhibitor cocktail, EDTA-free (78437, ThermoFisher)) for 15 min at 4°C with continuous mixing to demembranate cells and remove the sarcoplasmic reticulum, sarcolemma, and other organelles leaving the exposed myofilament network. Permeabilized myocyte preparations were then rinsed to remove detergents and individual myocyte preparations were selected on the basis of size (~50 - 200 μm in length) for mounting between a force transducer (Model 403A series; Aurora Scientific, Inc., Aurora, ON, Canada) and a high-speed motor (Model 315C-I; Aurora Scientific, Inc., Aurora, ON, Canada) using aquarium sealant (Aquarium sealant, Corning) to fix the ends of the cells to the motor and transducer. Push-button micromanipulators with submicron capability were used to adjust the position of the force transducer and

motor above a temperature-controlled platform (Model 803B Aurora Scientific) regulated by (825A, Aurora Scientific) Thermocouple, placed on the stage of an inverted microscope (Model 1X-71, Olympus Instrument Co., Japan). After glue curing, myocyte sarcomere length was adjusted to ~2.25 μm and force measurements were made at 15ºC by activating myocytes in pCa solutions containing variable free Ca^{2+} from pCa 9.0 to 4.5 as described previously[68]. Isometric force measurements (P) were normalized to maximum active force (P_0) at pCa 4.5 and subsequently graphed and fitted in Graphpad Prism using a Sigmoidal 4 parameter logistic curve where the given EC_{50} represents the pCa_{50} value for a given experiment. Rate of force redevelopment (k_{tr}) was calculated by fitting force traces with a single exponential curve, $t_{1/2}$ rate calculations at each pCa value (k) was normalized to maximum active rate measured at pCa 4.5 (k_0) for each measurement and then plotted against isometric force.

Videos of myocytes activated at submaximal [Ca^{2+}] near the pCa_{50} for force development were captured using an iPad and edited with Final Cut Pro Software (www.apple.com). Videos were subsequently analyzed using speckle tracking video analysis using open source Tracker 5.0.7 software[69] and vector movement representations were drawn using PIVLab analysis application in MATLAB[70,71] as shown in Figure 5 (main article text).

Statistics. All values represent the Mean ± SEM unless otherwise indicated. For echocardiography a one-way ANOVA was first used to determine if there were differences amongst groups based on sex or different founder lines. Because neither sex nor founder lines showed significant differences within their groups: male and female mice were grouped, and founder lines were grouped, then echocardiography results were analyzed for differences based on genotype alone. A two-way ANOVA was used to compare WT, HT, and HO Spy-C mice over time. A Tukey's post-hoc multiple comparisons test was used to determine significant differences (*$p<0.0332$) between groups. For force measurements, a minimum of 4-5 mice per group were used for all experiments. Group sizes were estimated based on previously published data sets

showing statistically significant differences at $p < 0.05$[34,68]. Data sets were tested for normality in GraphPad Prism using a Kolmogorov-Smirnov test. Quantile-Quantile plots were also generated to visually confirm normality as a linear relationship between quantiles. A repeated measures one-way ANOVA was used to compare force values at baseline (before treatment), after TEVp treatment, and after ligation of recombinant N'- terminal domains. A Tukey's post-hoc multiple comparisons test was used to determine significant differences (*p<0.0332) between these groups. Statistical analyses of all data sets were performed with Graphpad Prism Version 8.2.1.

Permeabilized myocyte sample preparation +/-TEVp for mass spec analyses. Left ventricles from 5 HO Spy-C mice were homogenized in skinning solution as described for force measurements. Tissue was washed three times in washing solution (1x isolation relax, 0.1% triton, 0.01% saponin), then once in 1x isolation-relax. Tissue from each mouse was split into TEV+ and TEV- samples. TEV+ samples were brought to 20 uM TEVp and incubated for 30 min at RT. Washing was done 3x with washing solution then resuspended in a clean tube with 250 uL isolation-relax. 250 uL 2x RIPA and 40 uL 20% SDS was added. Solutions were vortexed vigorously 3 times over 30 min at RT. Samples were centrifuged at 12k g for 5 min. Sample concentration was determined by BCA assay.

In-solution tryptic digestion of samples treated +/-TEVp. To determine changes in the sarcomeric proteome associated with TEVp digestion, 100 μg of myocyte homogenates from TEVp treated and TEVp untreated samples were supplemented with 6 volumes of pre-chilled 100% acetone and incubated one hour at -20°C to precipitate proteins followed by centrifugation at 16,000 x g for 10 minutes at 4°C. 400 μL of pre-chilled 90% acetone was added to the protein pellet and vortexed followed by centrifugation at 16,000 x g for 5 minutes at 4°C. The remaining acetone was removed and the protein pellets were air dried for 2-3 minutes. The protein pellet was resuspended in 100 μL of Digestion Buffer (50 mM NH_4HCO_3, 1% SDC) and sonicated for 5 minutes, supplemented with DTT at a final concentration of 5 mM and incubated at

56°C for 30 minutes. Samples were cooled to room temperature for 10 minutes and incubated with 15 mM acrylamide for 30 minutes at room temperature while protected from light. The samples were supplemented with additional DTT at a final concentration of 5 mM and incubated in the dark for 15 minutes to quench the alkylation reaction. 1 µg of Lys-C was added to each sample and incubated at 37°C for 2 hours while shaking at 300 rpm. Afterwards, 50 µL of 50 mM ammonium bicarbonate and 2 µg of trypsin was added to each sample and incubated at 37°C overnight while shaking at 300 rpm. 14.7 µL of 40% FA/1% HFBA was added to each sample and incubated for 10 minutes (final concentration is 4% FA/0.1% HFBA) to simultaneously stop trypsin digestion and cause precipitation of the SDC contained in the digestion buffer. The SDC was pelleted by centrifuging at 12,000 x g for 10 minutes and the peptide-containing solution was extracted. The samples were desalted with Pierce Peptide Desalting Spin Columns per the manufacturer's protocol (Thermo Scientific, cat no. 89852) and the peptides were dried by vacuum centrifugation. The dried peptides were resuspended in 20 µL of 0.1% FA (v/v) and the peptide concentration was determined with the Pierce Quantitative Colorimetric Peptide Assay Kit per the manufacturer's protocol (Thermo Scientific, cat no. 23275). 1 µg of the final sample was analyzed by mass spectrometry.

Mass spectrometry and data processing. HPLC-ESI-MS/MS was performed in positive ion mode on a Thermo Scientific Orbitrap Fusion Lumos tribrid mass spectrometer fitted with an EASY-Spray Source (Thermo Scientific, San Jose, CA). NanoLC was performed using a Thermo Scientific UltiMate 3000 RSLCnano System with an EASY Spray C18 LC column (Thermo Scientific, 50cm x 75 µm inner diameter, packed with PepMap RSLC C18 material, 2 µm, cat. # ES803); loading phase for 15 min at 0.300 µL/min; mobile phase, linear gradient of 1–34% Buffer B in 119 min at 0.220 µL /min, followed by a step to 95% Buffer B over 4 min at 0.220 µL /min, hold 5 min at 0.250 µL/min, and then a step to 1% Buffer B over 5 min at 0.250 µL /min and a final hold for 10 min (total run 159 min); Buffer A = 0.1% FA/H_2O; Buffer B = 0.1% FA in 80% ACN. All solvents were liquid chromatography mass spectrometry grade. Spectra were acquired using XCalibur, version 2.3 (Thermo Scientific). A "top speed" data-dependent MS/MS analysis

was performed. Dynamic exclusion was enabled with a repeat count of 1, a repeat duration of 30 sec, and an exclusion duration of 60 sec. Tandem mass spectra were extracted from Xcalibur 'RAW' files and charge states were assigned using the ProteoWizard 2.1.x msConvert script using the default parameters[72]. The fragment mass spectra were then searched against the *Mus musculus* SwissProt_2018_01 database (16965 entries) using Mascot (Matrix Science, London, UK; version 2.6) using the default probability cut-off score. The search variables that were used were: 10 ppm mass tolerance for precursor ion masses and 0.5 Da for product ion masses; digestion with trypsin; a maximum of two missed tryptic cleavages; variable modifications of oxidation of methionine and phosphorylation of serine, threonine, and tyrosine. Cross-correlation of Mascot search results with X! Tandem was accomplished with Scaffold (version Scaffold_4.8.7; Proteome Software, Portland, OR, USA). Probability assessment of peptide assignments and protein identifications were made through the use of Scaffold. Only peptides with ≥ 95% probability were considered. Reported peptide FDR rates from Scaffold ranged from 0.1-0.2%.

Label-free Quantitative Proteomics. Progenesis QI for proteomics software (version 2.4, Nonlinear Dynamics Ltd., Newcastle upon Tyne, UK) was used to perform ion-intensity based label-free quantification as previously described[73]. In Progenesis QI for Proteomics, peaks are identified and peak models are created that retain all relevant quantification and positional information. Protein abundance is calculated from corresponding peptide ion abundance values (using peptides that are not also part of another protein hit). In an automated format, .raw files were imported and converted into two-dimensional maps (y-axis = time, x-axis =m/z) followed by selection of a reference run for alignment purposes. An aggregate data set containing all peak information from all samples was created from the aligned runs, which was then further narrowed down by selecting only +2, +3, and +4 charged ions for further analysis. The samples were then grouped in TEVp treated versus TEVp untreated samples. 1 sample from the TEVp untreated group was discarded due to poor quality 2D chromatographs after repeated column runs. A peak list of fragment ion spectra was exported in Mascot generic file (.mgf) format and searched against the *Mus musculus* SwissProt_2018_01 database (16965 entries) using Mascot (Matrix Science, London, UK;

version 2.6). The search variables used were: 10 ppm mass tolerance for precursor ion masses and 0.5 Da for product ion masses; digestion with trypsin; a maximum of two missed tryptic cleavages; variable modifications of oxidation of methionine and phosphorylation of serine, threonine, and tyrosine; 13C=1. The resulting Mascot .xml file was then imported into Progenesis, allowing for peptide/protein assignment, while peptides with a Mascot Ion Score of <25 were not considered for further analysis. Precursor ion-abundance values for peptide ions were normalized to all proteins. A complete list of identified proteins and peptide ions can be found in Online Tables IV and V, respectively. Statistical analysis between TEVp treated and untreated samples was performed by Progenesis using a t-test.

ONLINE FIGURES

Online Figure I

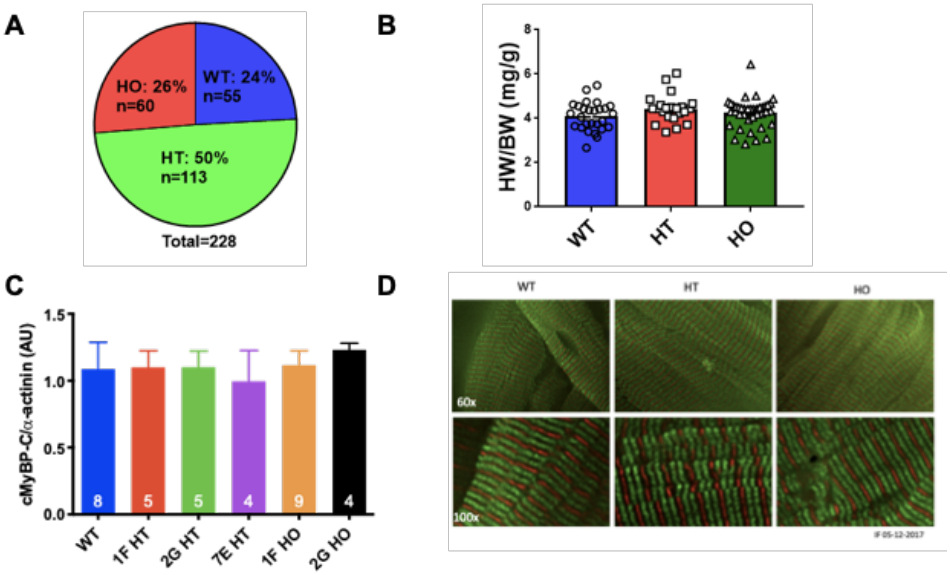

Online Figure I. Normal Mendelian inheritance and cMyBP-C expression in Spy-C mice. A) Spy-C mice were born in expected 1WT:2HT:1HO ratios from HT x HT crosses. **B)** Heart weight (HW) to body weight (BW) ratios were similar for WT, HT, and HO Spy-C mice. **C)** Summary data from western blots showing that cMyBP-C expression normalized to α-actinin was not significantly different in myocytes from WT, HT, or HO Spy-C mice. **D)** Immunofluorescence staining of representative WT, HT, and HO myocytes showing normal cMyBP-C (green doublets) and α-actinin (red) localization.

Online Figure II

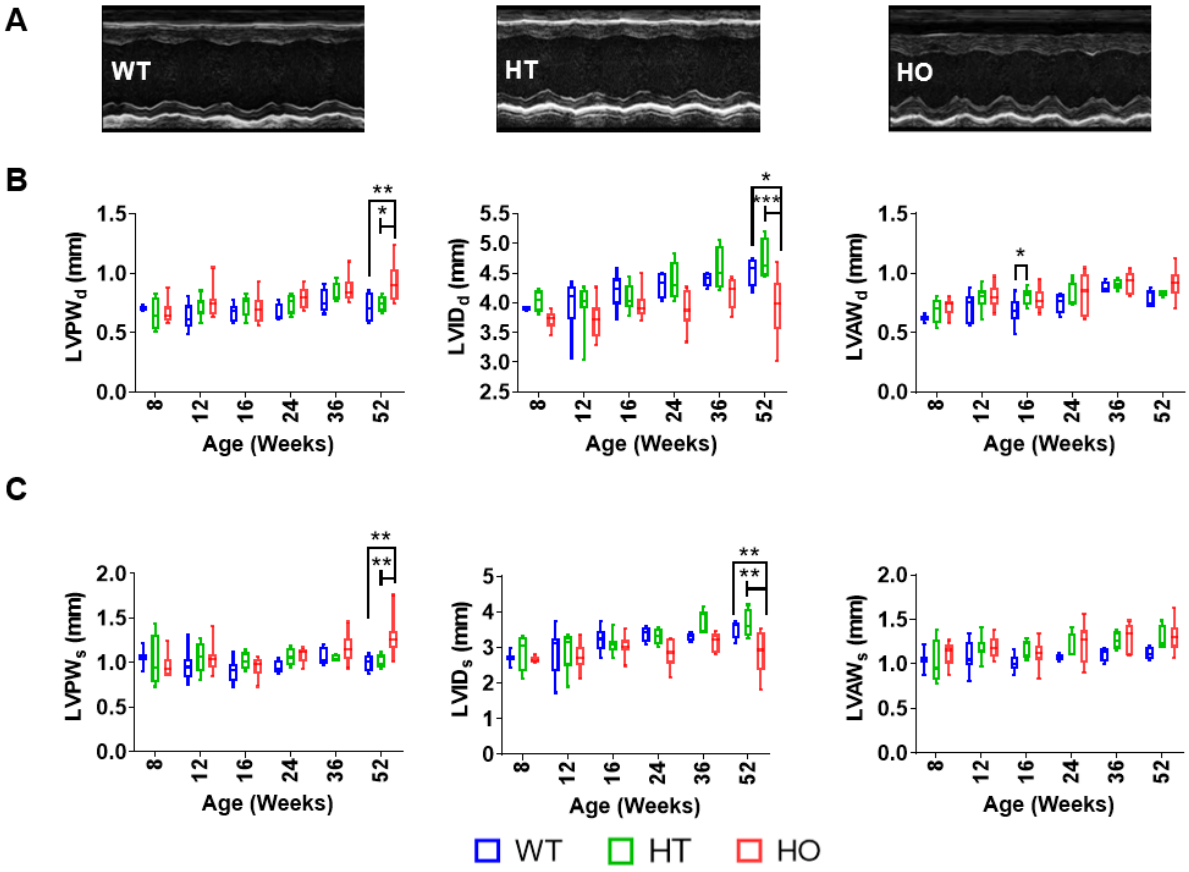

Online Figure II. Cardiac dimensions measured from echocardiography for WT (N=2-9), HT (N=4-11), and HO (N=6-12) Spy-C mice at 8-52 wks of age. A) Representative parasternal long axis one-dimensional M-Mode images from mice at 16 weeks of age. **B)** Diastolic LVPW, LVID, and LVAW wall dimensions. **C)** Systolic LVPW, LVID, and LVAW wall dimensions. See Online Table I for abbreviations. * p< 0.0332; ** p< 0.00221, *** p< 0.0002.

Online Figure III

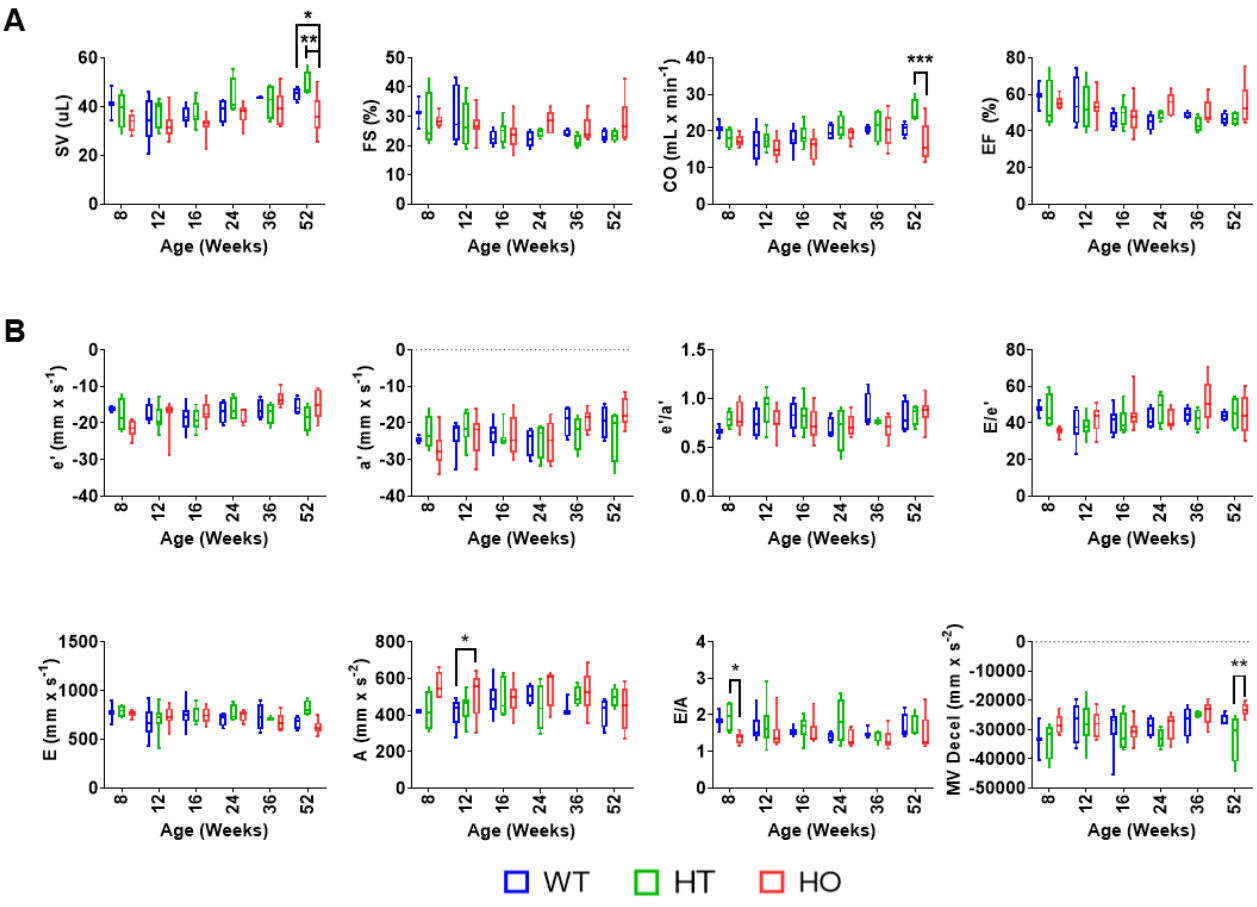

Online Figure III. Cardiac functional parameters determined from echocardiography of WT (N=2-9), HT (N=4-11), and HO (N=6-12) Spy-C mice at 8-52 wks of age. A) Systolic indices (SV, FS%, CO, and EF%). **B)** Diastolic indices obtained using pulse-wave Doppler imaging. See Online Table I for abbreviations. * $p< 0.0332$; ** $p< 0.00221$, *** $p< 0.0002$.

Online Figure IV

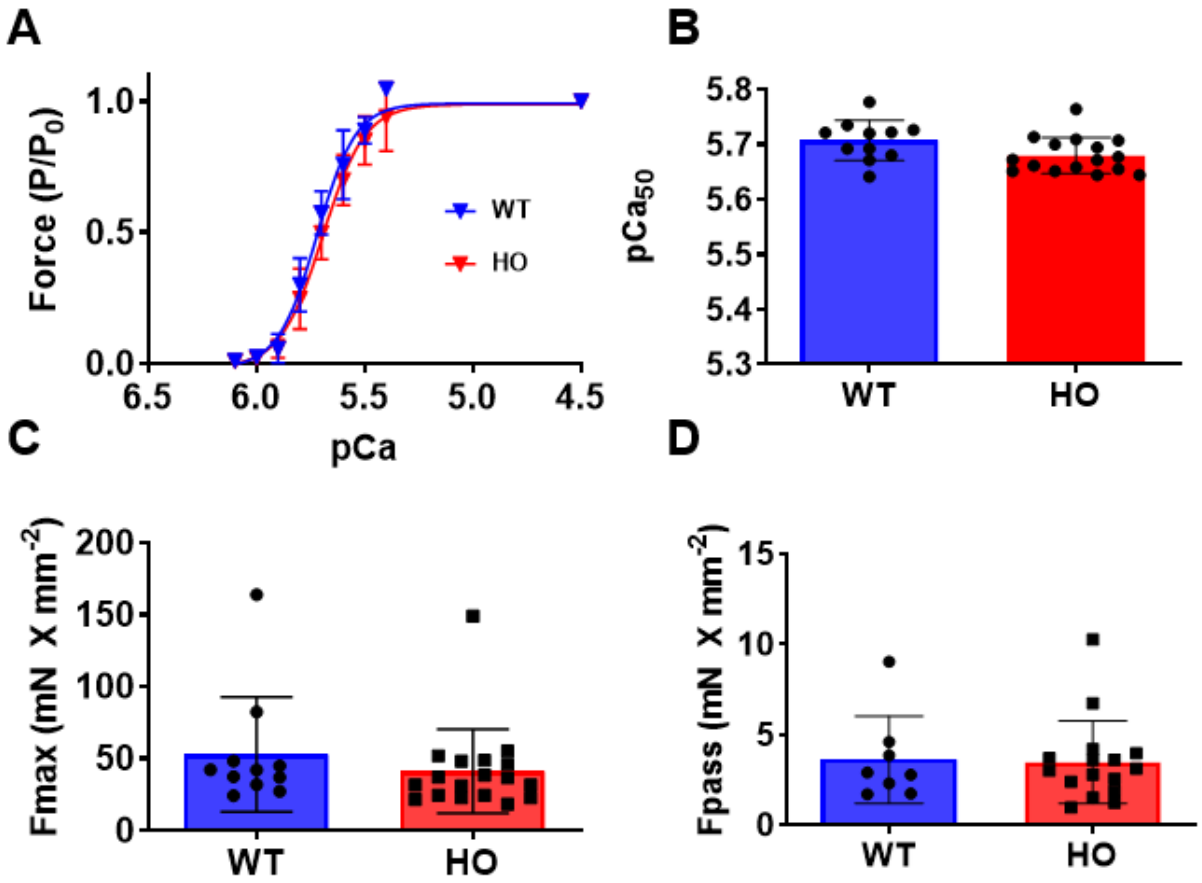

Online Figure IV. Active and passive steady state forces in myocytes from WT and HO Spy-C mice. A) Force-pCa curves showing similar tension-pCa relationships in WT and HO myocytes. **B)** Summary data from tension-pCa relationships showing pCa_{50} values were not significantly different for WT and HO myocytes (5.71 ± 0.01, n=11 and 5.68 ± 0.01, n=16 for WT and HO myocytes, respectively). **C)** Maximal Ca^{2+}-activated force (F_{max} at pCa 4.5) and **D)** passive force (F_{pas} at pCa 9.0) were not different between WT and HO myocytes.

Online Figure V

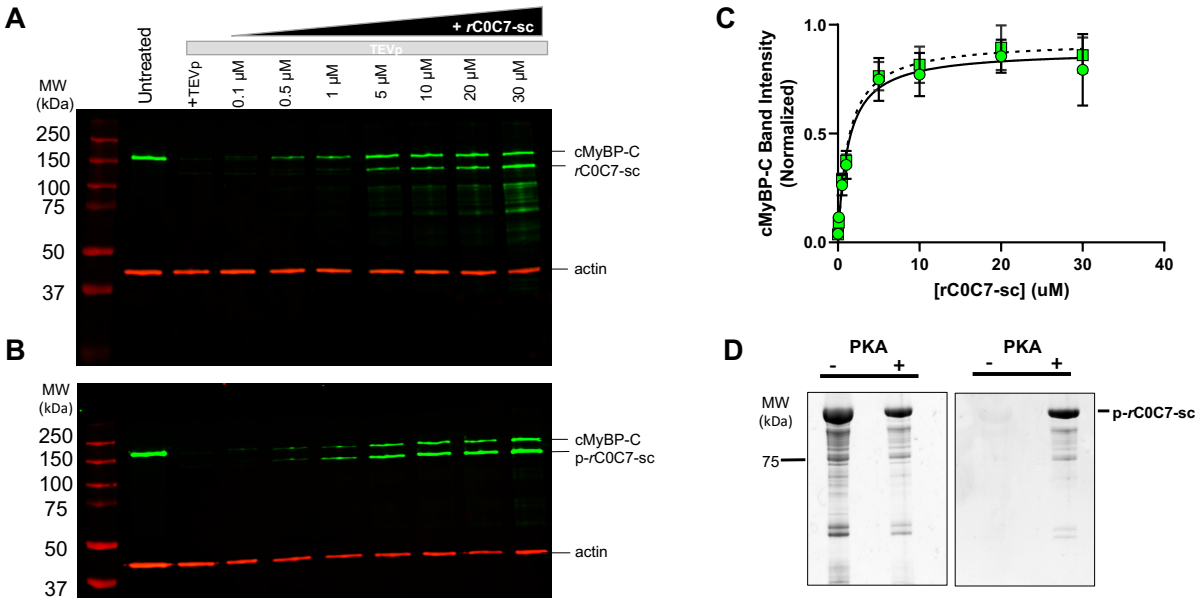

Online Figure V. Ligation efficiency of *r*C0C7-sc and phosphorylated *r*C0C7-sc in HO myocytes from Spy-C mice. Representative western blots showing LV homogenates before and after TEVp treatment and after covalent bond formation with increasing **A)** [*r*C0C7-sc] or **B)** phosphorylated [p-*r*C0C7-sc]. Homogenates were probed with an antibody against cMyBP-C[3]. Uncut cMyBP-C is visible as a band (green) in the untreated lane (far left). Newly ligated *r*C0C7-sc-st-C8C10 or p-*r*C0C7-sc-st-C8C10 is visible as a high molecular weight band (green) in lanes with added *r*C0C7-sc or p-*r*C0C7-sc. Excess (un-ligated) *r*C0C7-sc or p-*r*C0C7-sc is visible as a lower molecular weight band (green) below cMyBP-C. Actin (red) served as a loading control. **C)** Summary data from densitometric analysis of western blots as in A and B to quantify *r*C0C7-sc (circles) and p-*r*C0C7-sc (squares) ligation. The cMyBP-C/actin ratio in each lane was normalized to the cMyBP-C/actin ratio in the untreated lane which was taken as 1. Data show that ~90% ligation was achieved relative to uncut cMyBP-C using either [*r*C0C7-sc] or [p-*r*C0C7-sc] >10 µm. **D)** Phosphorylation of p-*r*C0C7-sc was confirmed by Pro-Q staining. *Left* panel: SyproRuby stained SDS-PAGE of *r*C0C7-sc before and after *in vitro* phosphorylation with PKA. *Right* panel: ProQ Diamond stained SDS-PAGE of *r*C0C7-sc before and after *in vitro* phosphorylation with PKA.

Online Figure VI

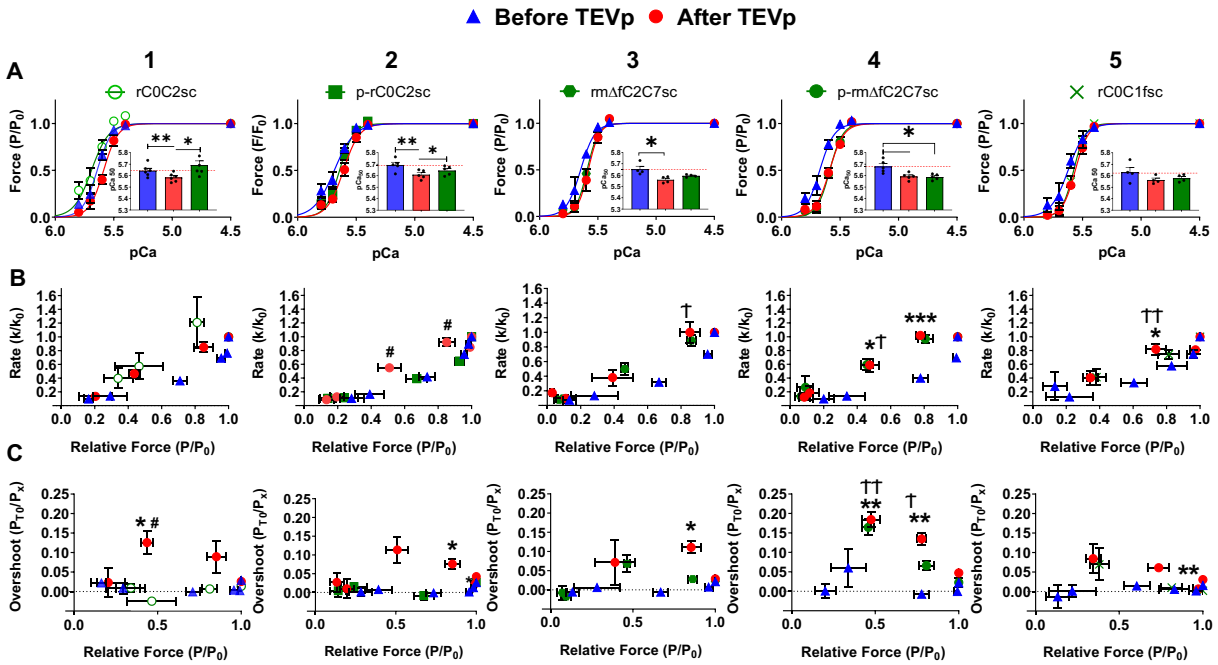

Online Figure VI. Summary of force measurements in HO myocytes before and after treatment with TEVp and after ligation with *r*C0C2-sc, p-*r*C0C2-sc, *r*mΔfC2C7-sc, p-*r*mΔfC2C7-sc, or *r*C0C1f-sc. 1A-5A). Summary isometric force data for HO myocytes showing increased Ca^{2+} sensitivity after treatment with TEVp for all experiments. After replacement with respective protein (1-5) indicated in the top column, both *r*C0C2-sc and p-*r*C0C2-sc restored Ca^{2+} sensitivity, but the effect was blunted with p-*r*C0C2-sc. Partial fragments lacking the first four domains of cMyBP-C (C0-P/A-C1-m) i.e: *r*mΔfC2C7-sc, p-*r*mΔfC2C7-sc, or *r*C0C1f-sc had no effect on Ca^{2+} sensitivity of tension. **1B-5B)** Summary k_{tr} data for HO myocytes before and after treatment with TEVp and after ligation with respective protein. After TEVp treatment k_{tr} increased at submaximal pCa values near the pCa_{50} values for force development. k_{tr} remained elevated following ligation with *r*C0C2-sc, but was reduced by p-*r*C0C2-sc. *r*mΔfC2C7-sc, p-*r*mΔfC2C7-sc, and *r*C0C1f-sc had no effect on k_{tr}. **1C-5C)** Force overshoots (P_{T0}) in HO myocytes expressed as a percentage over steady state force (P_x) (see Figure 4 for overshoot description). Force overshoots after TEVp treatment were most

common during activation at sub-maximal pCa_{50}. Overshoots were eliminated by *r*C0C2-sc and p-*r*C0C2-sc, but not by *r*mΔfC2C7-sc, p-*r*mΔfC2C7-sc, or *r*C0C1f-sc. Before TEVp vs. After TEVp: *p< 0.0332; **p< 0.00221, After TEVp vs. After ligation # p< 0.0332. Before TEVp vs. After ligation: ŧp< 0.0332, ŧ ŧp<0.00221.

Online Figure VII

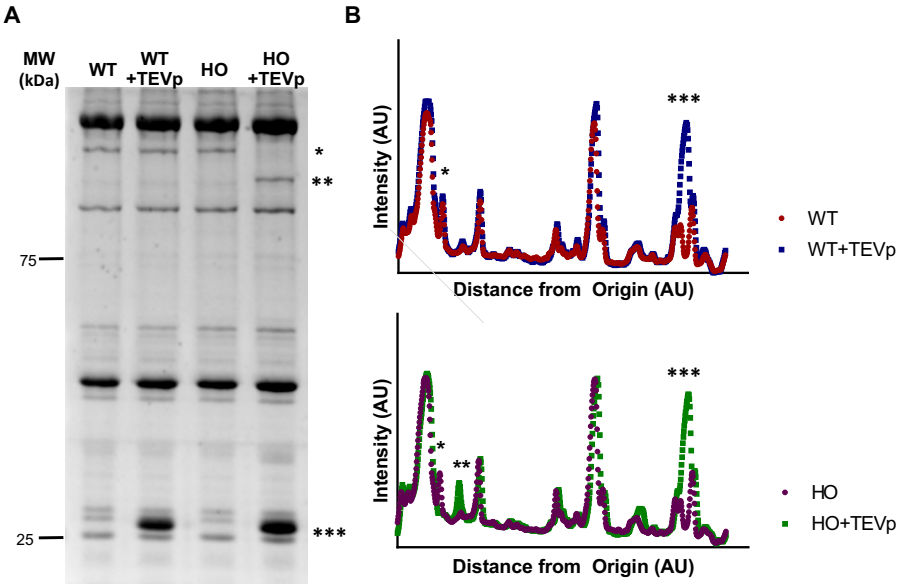

Online Figure VII. SDS-PAGE analysis of sarcomeric proteins in WT and HO myocytes before and after TEVp treatment. A) Representative SDS-PAGE of TEVp treated skinned myocytes from WT and HO Spy-C mice. Only cMyBP-C (*) in HO mice appears affected by TEVp (***) treatment, resulting in the appearance of the γC0C7 digestion product (**). **B)** Line scan analysis showing band intensity of the lanes of the gel in panel A. A single new band is seen corresponding to the expected γC0C7 (**) cleavage product. TEVp (~28 kDa) is observed in treated samples (***).

Online Figure VIII.

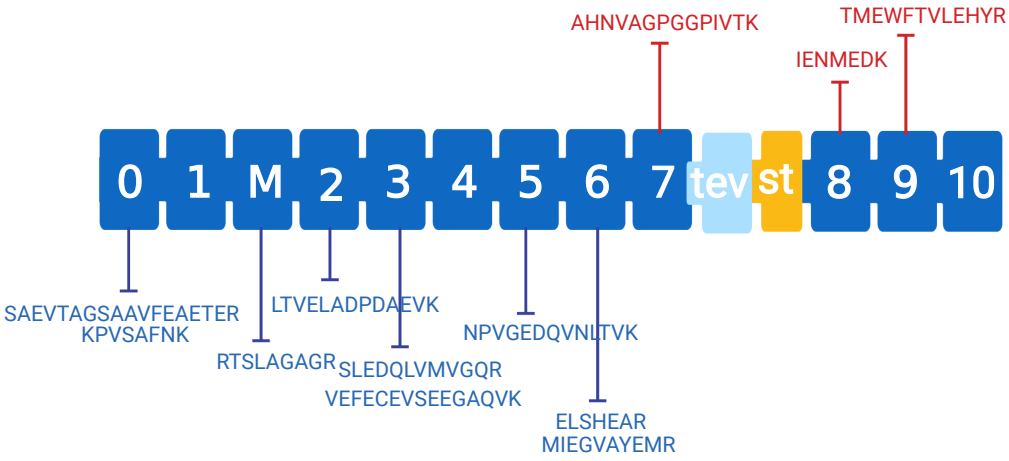

Online Figure VIII. Quantitative proteomics results showing a peptide ion map of significantly affected cMyBP-C peptide ions following TEVp treatment and washout. Quantitative proteomics identified a total of 849 proteins in samples from permeabilized HO myocytes treated with TEVp and untreated samples (N=5, N=4, respectively). Of the 849 proteins identified, 23 (2.7%) were found to be significantly different between the TEVp treated and untreated samples, with 8 (1%) decreased in abundance and 15 (1.8%) increased (See Online Tables IV and V for a complete list of proteins and peptide ions identified, respectively). cMyBP-C (*MYBPC3*) was the most significantly affected out of all proteins identified ($p < 0.0006$) with a decrease in abundance following TEVp cleavage. The only other sarcomeric protein identified was titin which showed a significant increase in abundance in TEVp treated samples ($p < 0.037$). The anomalous increase in titin abundance may be due to an unmasking effect from loss of cMyBP-C. For cMyBP-C, 416 total peptide ions were identified with 48 (12%) significantly decreased in TEVp treated samples and 6 (1.5%) significantly increased in TEVp treated samples. Shown plotted above are peptide ions (*blue*) that were consistently decreased in 2 or more of the treated samples (9 peptide ions). All mapped to the N'-terminal C0C7 domains of cMyBP-C as expected for loss of γC0C7 domains following TEVp cleavage and washout. Peptide ions that were significantly increased (*red*) in 2 or more

samples mapped to the C'-terminus of the molecule near the TEVp cut site. A similar analysis for titin showed that 88 of 3325 (2.6%) total peptide ions were significantly affected, with 65 significantly increased while 23 were significantly decreased. Of those that decreased in 2 or more TEVp treated samples (4 peptide ions), the distribution appeared random and the position of peptide ions was not correlated with a TEVp consensus sequence (not shown). Taken together, these data support the high specificity of TEVp treatment to selectively reduce Spy-C cMyBP-C in HO sarcomeres without causing significant loss of other sarcomeric proteins. Summary of data can be found in linked Online Tables IV-V.

Online Table I: Abbreviations of Echocardiography Measurements

Abbreviation	Description
LVIDd and LVIDs	Left ventricular internal diameter diastolic and systolic
LVAWd and LVAWs	Left anterior wall thickness diastolic and systolic
LVPWd and LVPWs	Left ventricular peripheral wall thickness diastolic and systolic
HR	Heart rate
SV	Stroke volume
EF	Ejection fraction
FS	Fractional shortening
CO	Cardiac output
E	Peak velocity of blood flow into the LV during early diastole
A	Peak velocity of blood flow into the LV during atrial contraction
e'	Peak velocity of tissue movement at the mitral annulus during early diastole
a'	Peak velocity of tissue movement at the mitral annulus during atrial contraction
MV decel	Mitral valve deceleration

Online Table II: Summary force data before and after TEVp treatment, and after ligation with indicated recombinant proteins.

Genotype	*Protein (N, n)*	*Before TEVp*	*After TEVp*	*After Protein*
WT	*r*C0C7-sc (5, 11)	5.59 ± 0.021	5.59 ± 0.018	5.59 ± 0.016
	p-*r*C0C7-sc (4, 4)	5.67 ± 0.033	5.67 ± 0.033	5.63 ± 0.024
HO	*r*C0C7-sc (5, 7)	5.59 ± 0.010	5.52 ± 0.010***###	5.59 ± 0.015
	p-*r*C0C7-sc (7, 8)	5.61 ± 0.016	5.56 ± 0.010***	5.55 ± 0.018ŦŦŦ
	*r*C0C2-sc (6, 6)	5.64 ± 0.021	5.58 ± 0.015**#	5.69 ± 0.036
	p-*r*C0C2-sc (5, 5)	5.69 ± 0.024	5.61 ± 0.017#	5.65 ± 0.017
	*r*m**Δf**C2C7-sc (4, 4)	5.65 ± 0.027	5.56 ± 0.013*	5.59 ± 0.0060
	p-*r*m**Δf**C2C7-sc (5, 5)	5.68 ± 0.025	5.59 ± 0.013*	5.58 ± 0.011Ŧ
	*r*C0C1f-sc (4, 4)	5.63 ± 0.04	5.56 ± 0.016	5.54 ± 0.016

Fpas (mN x mm^{-2})

Genotype	Protein (N, n)	Before TEVp	After TEVp	After Protein
WT	*r*C0C7-sc (5, 11)	3.96 ± 1.77	4.41 ± 1.97	4.91 ± 2.19
	p-*r*C0C7-sc (4, 4)	5.62 ± 2.81	5.43 ± 2.71	5.29 ± 2.65
HO	*r*C0C7-sc (5, 7)	2.86 ± 0.98	3.32 ± 1.26	3.58 ± 1.35
	p-*r*C0C7-sc (7, 8)	4.41 ± 1.56	4.22 ± 1.49	4.76 ± 1.68
	*r*C0C2-sc (6, 6)	2.21 ± 0.62	2.16 ± 0.66	3.38 ± 1.34
	p-*r*C0C2-sc (5, 5)	3.50 ± 1.05	4.10 ± 1.23	3.92 ± 1.31
	*r*m**Δf**C2C7-sc (4, 4)	2.00 ± 1.00	2.02 ± 1.01	2.16 ± 1.08
	p-*r*m**Δf**C2C7-sc (5, 5)	2.67 ± 1.34	2.82 ± 1.41	3.23 ± 1.61
	*r*C0C1f-sc (4, 4)	2.90 ± 1.26	3.05 ± 1.30	3.53 ± 1.64

Fmax (mN x mm^{-2})

Genotype	Protein (N, n)	Before TEVp	After TEVp	After Protein
WT	*r*C0C7-sc (5, 11)	49.59 ± 22.18	43.03 ± 19.24	36.88 ± 16.49
	p-*r*C0C7-sc (4, 4)	57.47 ± 28.74	46.89 ± 23.45	41.75 ± 20.88
HO	*r*C0C7-sc (5, 7)	38.46 ± 14.50	30.47 ± 11.51	26.8 ± 10.14
	p-*r*C0C7-sc (7, 8)	54.19 ± 19.16	45.11 ± 15.94	37.86 ± 13.38
	*r*C0C2-sc (6, 6)	32.14 ± 8.00	24.90 ± 7.22*	21.44 ± 6.52Ŧ
	p-*r*C0C2-sc (5, 5)	44.0 ± 8.71	35.8 ± 6.57*##	30.6 ± 6.64ŦŦ
	*r*m**Δf**C2C7-sc (4, 4)	31.90 ± 15.98	24.85 ± 12.42*	22.00 ± 11.00Ŧ
	p-*r*m**Δf**C2C7-sc (5, 5)	53.63 ± 25.94	43.87 ± 19.96	39.55 ± 17.68
	*r*C0C1f-sc (4, 4)	52.60 ± 20.82	43.35 ± 17.96	43.25 ± 18.68

**Values are presented as Mean ± SEM Before TEVp vs. After TEVp: *p< 0.0332; **p< 0.00221, ***p< 0.0002, After TEVp vs. After ligation # p< 0.032. # # p< 0.00221. # # # p< 0.0002. Before TEVp vs. After ligation: ŧp< 0.0332, ŧŧp<0.00221, ŧŧŧp<0.0002*

Online Table III: Summary SPOC and force overshoots before and after TEVp treatment, and after ligation with recombinant proteins.

Genotype	Protein (N, n)	Overshoot at pCa_{50} (Before TEVp)	Overshoot at pCa_{50} (After TEVp)	Overshoot at pCa_{50} (After Protein)
WT	*r*C0C7-sc (5, 11)	×	×	×
	p-*r*C0C7-sc (4, 4)	×	×	×
HO	*r*C0C7-sc (5, 7)	×	✓	×
	p-*r*C0C7-sc (7, 8)	×	✓	✓
	*r*mΔfC2C7-sc (4, 4)	×	✓	✓
	p-*r*mΔfC2C7-sc (5, 5)	×	✓	✓
	*r*C0C1f-sc (4, 4)	×	✓	✓
Genotype	Protein (N, n)	SPOC at pCa_{50} (Before TEVp)	SPOC at pCa_{50} (After TEVp)	SPOC at pCa_{50} (After Protein)
WT	*r*C0C7-sc (5, 11)	×	×	×
	p-*r*C0C7-sc (4, 4)	×	×	×
HO	*r*C0C7-sc (5, 7)	×	✓	×
	p-*r*C0C7-sc (7, 8)	×	✓	✓
	*r*mΔfC2C7-sc (4, 4)	×	✓	✓
	p-*r*mΔfC2C7-sc (5, 5)	×	✓	✓
	*r*C0C1f-sc (4, 4)	×	✓	✓

✓ indicates observed × indicates not observed

Major Resources Table

In order to allow validation and replication of experiments, all essential research materials listed in the Methods should be included in the Major Resources Table below. Authors are encouraged to use public repositories for protocols, data, code, and other materials and provide persistent identifiers and/or links to repositories when available. Authors may add or delete rows as needed.

Animals (in vivo studies)

Genetically Modified Animals

	Species	Vendor or Source	Background Strain	Other Information	Persistent ID / URL
Parent – Male Spy-C	Mouse	University of Arizona GEMM Core	BL6/NJ	CRISPR/Cas 9 Edited	
Parent – Female Spy-C	Mouse	University of Arizona GEMM Core	BL6/NJ	CRISPR/Cas 9 Edited	

Antibodies

Target antigen	Vendor or Source	Catalog #	Working concentration	Lot # (preferred but not required)	Persistent ID / URL
Actin	Sigma-Aldrich (St. Louis, MO, USA)	A9357	1:5,000		
a-actinin	Sigma-Aldrich (St. Louis, MO, USA)	A7811	1:5,000		
cMyBP-C	Custom antibody (University of Wisconsin, Madison, WI)	Harris Lab	1:75,000	Reference: Harris et al, Circ Res 2002;90:594–601.	
Anti-Rabbit (2^0)	Li-Cor (Lincoln, Nebraska, USA)	800CW	1:10,000		
Goat Anti-Mouse (2^0)	Li-Cor (Lincoln, Nebraska, USA)	680CW	1:10,000		
a-actinin AlexaFluor568	Life Technologies (Thermo-Fisher)	A11004	1:10,000		
SpyTag	Genscript (Piscataway, NJ)	Custom antibody order/Harris Lab	1:10,000		

DNA/cDNA Clones

Clone Name	Sequence	Source	Persistent ID / URL
*r*C0C7sc (and related plasmids subcloned or modified from this template)	NP_032679.2 (mouse cMyBP-C cDNA sequence) *Sequence was codon optimized by Genscript for expression in bacteria.	GenScript (Piscataway, NJ)	
TEV protease, S219V mutant	pRK793	Addgene #8827	

Data & Code Availability

Description	Source / Repository	Persistent ID / URL
Data that support the findings of this study are available from the corresponding author upon reasonable request.	Harris Lab	

Online Video Legends

Online Video I (separate file). 3 activations of the same permeabilized HO Spy-C myocyte preparation in a submaximal pCa solution (near the pCa_{50} for force generation). *Left*, myocyte shown contracting at steady state force (at plateau) before treatment with TEVp; *Middle*, myocyte shown contracting at steady state force (at plateau) after treatment with TEVp. Note continuous oscillatory wave behavior (SPOC). *Right*, myocyte shown contracting at steady state force (at plateau) after ligation with *r*C0C7-sc. Note that all force oscillations are damped.

Online Video II (separate file): 3 activations of the same permeabilized HO Spy-C myocyte preparation in a submaximal pCa solution (near the pCa_{50} for force generation). *Left*, myocyte shown contracting at steady state force (at plateau) before TEVp treatment; *Middle*, myocyte shown contracting at steady state force (at plateau) after treatment with TEVp. Note persistent oscillatory wave behavior (SPOC); *Right*,

myocyte shown contracting at steady state force (at plateau) after ligation of p-*r*C0C7-sc. Note that oscillatory wave behavior is mostly damped, but SPOC is still visible.

Online Video III (separate file): 3 activations of the same permeabilized WT Spy-C myocyte preparation in a submaximal pCa solution (near the pCa_{50} for force generation). *Left*, myocyte shown contracting at steady state force (at plateau) before TEVp treatment; *Middle*, myocyte shown contracting at steady state force (at plateau) after treatment with TEVp. *Right*, myocyte shown contracting at steady state force (at plateau) after incubation with *r*C0C7-sc. Note the absence of SPOC under all conditions.

Online Video IV (separate file): 3 activations of the same permeabilized HO Spy-C myocyte preparation in a submaximal pCa solution (near the pCa_{50} for force generation). *Left*, myocyte shown contracting at steady state force (at plateau) before TEVp treatment; *Middle*, myocyte shown contracting at steady state force (at plateau) after treatment with TEVp. Note persistent oscillatory wave behavior (SPOC); *Right*, myocyte shown contracting at steady state force (at plateau) after ligation of *r*C0C2-sc. Note that all force oscillations are damped.

Online Video V (separate file): 3 activations of the same permeabilized HO Spy-C myocyte preparation in a submaximal pCa solution (near the pCa_{50} for force generation). *Left*, myocyte shown contracting at steady state force (at plateau) before TEVp treatment; *Middle*, myocyte shown contracting at steady state force (at plateau) after treatment with TEVp. Note persistent oscillatory wave behavior (SPOC); *Right*, myocyte shown contracting at steady state force (at plateau) after ligation of p-*r*C0C2-sc. Note that oscillatory wave behavior is mostly damped, but SPOC is still visible.

Online Video VI (separate file): 3 activations of the same permeabilized HO Spy-C myocyte preparation in a submaximal pCa solution (near the pCa_{50} for force generation). *Left*, myocyte shown contracting at steady state force (at plateau) before TEVp treatment; *Middle*, myocyte shown contracting at steady state

force (at plateau) after treatment with TEVp. Note persistent oscillatory wave behavior (SPOC); *Right*, myocyte shown contracting at steady state force (at plateau) after ligation of *r*-m□fC2C7-sc. Note that oscillatory wave behavior is mostly damped, but SPOC is still visible.

Online Video VII (separate file): 3 activations of the same permeabilized HO Spy-C myocyte preparation in a submaximal pCa solution (near the pCa_{50} for force generation). *Left*, myocyte shown contracting at steady state force (at plateau) before TEVp treatment; *Middle*, myocyte shown contracting at steady state force (at plateau) after treatment with TEVp. Note persistent oscillatory wave behavior (SPOC); *Right*, myocyte shown contracting at steady state force (at plateau) after ligation of *r*C0C1f-sc. Note that oscillatory wave behavior is mostly damped, but SPOC is still visible.